

# Microstrip Inset Fed Rectangular Dielectric Resonator Antenna for Near Field Communication

Sovan Mohanty  
Bareilly, India

Bahbaswata Mohapatra  
Greater Noida

**Article History:** Received: 10 November 2020; Revised 12 January 2021 Accepted: 27 January 2021; Published online: 5 April 2021

**Abstract:** Due to the availability of only limited dimensions of dielectric material, frequency tuning is very challenging in a dielectric resonator antenna. The objective is to enhance the tunability range of the DRA by altering the inductive inset feeding techniques. In this paper, novel low-profile rectangular dielectric resonator antennas with three different microstrip inset feeding mechanisms are studied and analyzed. It is observed that by varying the feeding techniques, the operating frequency can be easily altered, without significant variation in the impedance match. The dielectric waveguide model is used for approximate calculation of the dimension, and magnetic wall modelling is used for the overall analysis. The reflection coefficient, radiation pattern, co and cross-polarization, and gain are studied. The proposed antenna is resonating in the upper spectrum of the X band, and the lower spectrum of the Ku band with efficiency as high as 99%, a gain of 7 dBi, and the output pattern shows a broadside mode.

**Keywords:** Rectangular dielectric resonator antenna, Dielectric wave guide model, Perfect electrical conductor, Near field communication

## 1. Introduction

The operational carrier frequency of modern wireless technology has undergone a tremendous upward translation in the last decade to satisfy modern applications. The concentration is mainly to achieve high speed, wide bandwidth, polarization purity, high gain, high efficiency, high radiation stability, and low profile design. According to Edholm's law the required bandwidth and data rate doubles every eighteen months. Further, according to Shannon Hartley's theorem, high channel capacity can be obtained by operating the system at high frequency (**Ramo.S. et al.,1993**). It is because bandwidth is directly proportional to the frequency of operation. High-frequency design has to deal with time-variant, non-linear, non-homogeneous, nonisotropic behavior (**Harrington.R.F.,2001**). As the applied wavelength decreases and becomes comparable to the physical dimension of the device then phase reversal and transit time effect dominates. It means all the components and even transmission lines used for feeding the structure will behave as a resonant circuit, and overall behavior will be narrowband. The bandwidth handling capabilities of an antenna are usually being expressed by input impedance and frequency of operation. Bandwidth can also be expressed by output characteristics such as gain, cross-polarization level, beam width, etc.

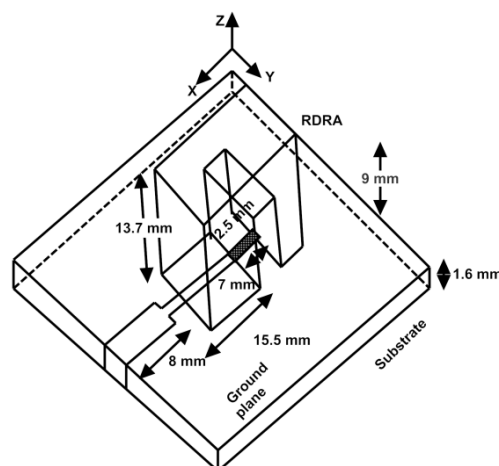
The most popular microstrip patch antenna is a capacitive narrow-band structure (**Pozar.D.M.,1995**). Therefore to fulfill the hungriness of the communication industry, especially in terms of high bandwidth, a dielectric resonator antenna is the ultimate choice (**Luk.K.M, et al.,2013**). It has a low dielectric loss, conductor loss, and radiation loss with desired polarization characteristics. Rectangular DRA offers the highest design flexibilities because of its three-dimensional structure with two degrees of freedom. The high sensitiveness of the antenna demands tight impedance matching. The matching techniques like quarter-wave transformers, stub matching, and Tchebyshev impedance networks can easily become compatible with DRA (**Mongia.R.K. et al., 1997**). However, DRA has got certain inherent limitations like unavailability of dielectric material with desired permittivity and dimension, difficulty in frequency tuning, high cost of the dielectric material, complicated fabrication process, unavailability of accurate numerical techniques, etc. Therefore practically designer faces difficulties to achieve precision and accuracy (**Coulibaly.Y.T. et al.,2008**).

In this paper, a novel RDRA having different microstrip inset feeding mechanisms is being proposed. The matching profile of this antenna is enhanced by concentrating the field underneath the DRA. Here three inset feeds are used to optimize the coupling and to enhance the bandwidth performance. DRA-I is fed by a 50 Ohm horizontal microstrip line, DRA-II is fed by a vertical microstrip feed at the beginning of an aperture, and DRA-III is fed by a vertical microstrip feed at the end of an aperture. DRA-I is considered to be magnetic field coupling whereas DRA-II & III are considered to be electric field coupling. The stub of the transmission line is adjusted to optimize the capacitive and inductive aspects of the matching profile. It is found that DRA-I is operating from 12.22 GHz to 13.84 GHz with a maximum resonant dip of -38 dB that occurs at 12.48 GHz. DRA-II is operating in two bands. The first band is from 10.54 GHz to 11.06 GHz with a maximum resonant frequency at 10.74 GHz (-23.55 dB). The second band is from 12.22 GHz to 12.96 GHz with resonant frequency at 12.74 GHz (-36.13 dB). DRA-III is operating from 10.86 GHz to 12.1 GHz with the maximum resonant frequency of 11.36 GHz (-58.8 dB). Because of the symmetrical field distribution, the radiation pattern in all these configurations is in a broadside direction. The rectangular DRA is radiating like a short horizontal magnetic dipole (Petosa.A.,2007). To optimize the proposed design parametric analysis was carried out by employing the finite element method (Garg.R.,2008).

The structure of the antenna is presented in Section II. A thorough parametric study is presented in Section III. The result analysis and discussion of various geometries is presented in Section IV. In the end, conclusions are given in Section V.

## 2. Structure of the Antenna

Figures 1a and 1b describe the detailed topology of the proposed DRA-I, DRA-II, and DRA-III. It consists of a rectangular dielectric resonator placed on a substrate below which an infinite ground plane is placed. The ground plane acts as an electrical wall in which the tangential component of the electric field is zero and the normal component of the electric field exists. The substrate made up of Roger TMM4 (tm),  $\epsilon_r = 4.5$ , loss tangent  $\tan \delta = 0.002$  having a dimension of  $50 \times 50 \times 1.6 \text{ mm}^3$ . The substrate is thin enough to reduce the induction of surface wave but it is mechanically strong enough to provide the required support. RDRA is made up of Rogers RT/Duroid 6010 with  $\epsilon_r = 10.2$ , and  $\tan \delta = 0.0023$ . The dimension of the RDRA is  $17.5 \times 4.94 \times 13.7 \text{ mm}^3$ . As shown in fig. 1a & b an aperture of dimension  $2.5 \times 4.94 \times 9 \text{ mm}^3$  is cut into the RDRA to decrease the quality factor and to improve the effective impedance bandwidth of the RDRA. Silicone sealant is used to join the substrate with the RDRA. An infinite ground plane as a perfect electrical conductor of dimension  $50 \times 50 \times 1.6 \text{ mm}^3$  is placed at the backside of the substrate to improve the front-to-back ratio. The antenna is excited by a microstrip transmission line because it permits easy integration of DRA with the microwave circuits (Yaduvanshi,R.S. et al.,2016). The dimension of the microstrip transmission line-I from the source side is  $4.94 \times 3 \text{ mm}^2$ . After that transmission line of various lengths but a width of 2mm is used to optimize the impedance matching. The DRA is placed over the maximum concentrated electric field of the feeding line (Mohanty.S. et al.,2020).



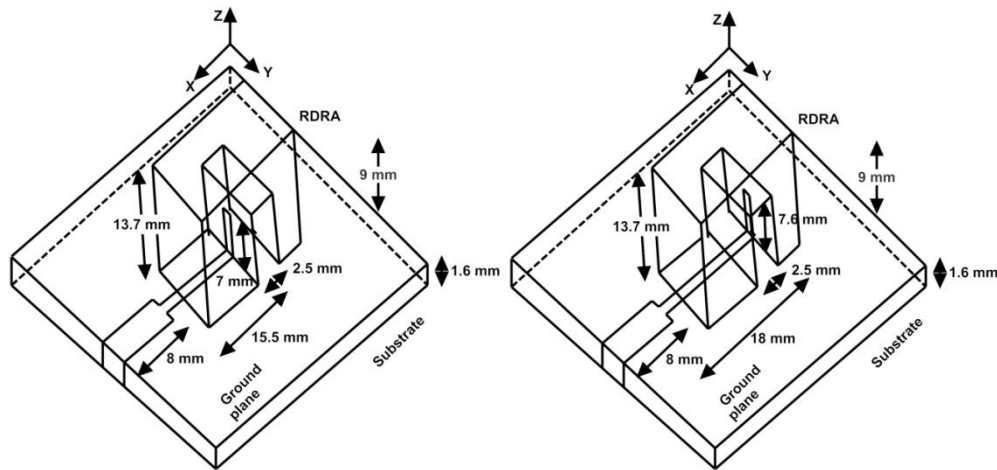


Figure 1a. Showing the side view of DRA-I, DRA-II, DRA-III.

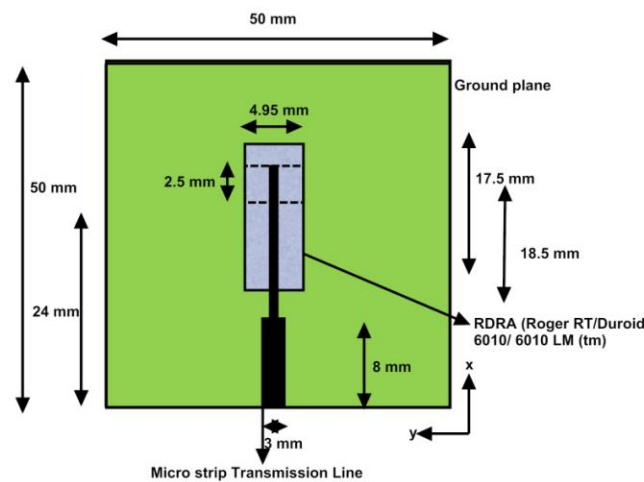


Figure 1b. Showing the top view of DRA-I.

Table 1. Showing the structural parameters of the RDRA

Structure	Length	Width	Height	Permittivity	Material	$\tan \delta$
Substrate	50 mm	50 mm	1.6 mm	4.5	Roger TMM4(tm)	0.002
DRA I,II, & III	17.5 mm	4.94 mm	13.7 mm	10.2	Roger RT/Duroid 6010/6010 LM (tm)	0.0023

### 3. Parametric Study

In this project parametric study is obtained from the DRA characteristics. Inserted DRA with the initial stub is used to enhance the bandwidth and the matching profile. The dimension of the stub such as width and length provides the capacitive and inductive effect. In DWM the upper surface and two side walls of the DRA are considered to be perfect magnetic walls and DRA is placed over the conducting ground plane and an electrical wall is present at the bottom surface. The field within the guide is sinusoidal whereas the field outside the guide is exponentially decaying in nature (Mongia.R.K. et al.,1997). It is essential to find the wave propagation number in x, y, z directions that is  $k_x, k_y, k_z$ , and attenuation constant in x and y directions. The wavenumber ‘k’ can be defined as phase shift per unit length i.e.  $k = \omega\sqrt{\mu\epsilon}$ . Without the presence of the source: The wave equation (vector) for the magnetic field is (Petosa.A.,2007):

$$\nabla^2 H + k^2 H = 0 \quad (1a)$$

The wave equation (vector) for the electric field is:  $\nabla^2 E + k^2 E = 0$  (1b)

Thus,  $E(\nabla^2 + k^2) = 0$ . In the x direction,  $E_x \left( \frac{\partial^2}{\partial z^2} + k^2 \right) = 0$  wave is moving in the z-direction. Solving

$$E_x = E e^{\pm jkz} \quad (2)$$

The negative sign is for describing the forward-travelling wave and the positive sign is to represent the backward travelling wave. If there is the presence of  $E_z$  and  $H_z$  components simultaneously in the z-direction, the generated field pattern is called Hybrid mode. The second-order partial differential equation is based on the equation of string. It is used to describe the characteristics of the wave. We retain that mathematical language to convey the characteristics of an antenna. In the presence of the source, DRA can be characterized by Helmholtz's equation. Helmholtz's equation is the sun in electromagnetic. The radiating fields can be calculated from the electric and magnetic current density. It is achieved by taking the route of potential functions. The potential function can be calculated through scalar manipulations to avoid complicated vector manipulation. Electric and magnetic vector potentials are manmade quantities (**Harrington.R.F.,2001**).

$$\nabla^2 A + k^2 A = -J \quad (3a)$$

$$\nabla^2 F + k^2 F = -M \quad (3b)$$

F= Electric vector potential, A= Magnetic vector potential. The field distribution is determined by the DWM assuming that the DRA is placed on infinite ground planes. In an RDRA with dimensions length 'a' (major axis), width 'b' (minor axis), and height 'd', having a, b>d, the dominant mode will be  $TE_{11\delta}^z$ . By using the DWM following field will be obtained within the DRA which is basically sinusoidal in nature (**Luk.K.M, et al.,2013**).

$$H_x = \frac{(k_x k_z)}{j\omega\mu_0} \sin(k_x x) \cos(k_y y) \sin(k_z z) \quad (4)$$

$$H_y = \frac{(k_y k_z)}{j\omega\mu_0} \cos(k_x x) \sin(k_y y) \sin(k_z z) \quad (5)$$

$$H_z = \frac{(k_x^2 + k_z^2)}{j\omega\mu_0} \cos(k_x x) \cos(k_y y) \cos(k_z z) \quad (6)$$

$$E_x = k_y \cos(k_x x) \sin(k_y y) \cos(k_z z) \quad (7)$$

$$E_y = -k_x \sin(k_x x) \cos(k_y y) \cos(k_z z) \quad (8)$$

$$E_z = 0 \quad (9)$$

$$k_x^2 + k_y^2 + k_z^2 = \epsilon_r k_0^2 \quad (10)$$

$$\sqrt{k_0^2(\epsilon_r - 1) - k_z^2} \quad k_z \tan\left(\frac{k_z d}{2}\right) = \quad (11)$$

$$k_x = \frac{m\pi}{a} \quad (11a)$$

$$k_y = \frac{n\pi}{b} \quad (11b)$$

The value of  $\delta$  in the lowest order mode is given by:

$$\delta = \frac{k_z}{\pi/d} \quad (12)$$

The obtained field structure is very much similar to the field produced by the short magnetic dipole. The radiated power P will be:

$$P = \int_0^a \int_0^b (E \times H^*) dx dy \quad (13)$$

$$P = P_r + jP_i \quad (14)$$

$P_r$  = Radiated power due to dominant mode

$P_i$  = Imaginary power due to higher order mode

Imaginary part  $P_i$  has to be nullified. So we have to find  $50 \Omega$  point sacrificing efficiency. Thus point of excitation is very sensitive and should be independent of the types of mode whether TE or TM. Designer interest lies in the selection of single mode to carry the power. A degenerate counterpart of TE01 is TM01 which in practice does not exist. Thus if we will work at higher mode then we have to ensure that lower order does not exist. Thus we have to use a mode suppressor. According to the DWM method (Petosa.A.,2007).:

$$k_x^2 + k_y^2 + k_z^2 = \epsilon_r k_0^2 \tag{15}$$

$$\left(\frac{m\pi}{a}\right)^2 + \left(\frac{n\pi}{b}\right)^2 + k_z^2 = \epsilon_r k_0^2 \tag{16}$$

$$k_z^2 = \epsilon_r k_0^2 - \left(\frac{m\pi}{a}\right)^2 - \left(\frac{n\pi}{b}\right)^2 \tag{17}$$

Putting the value of  $k_z$  in the below given equation

$$k_z \tan\left(\frac{k_z d}{2}\right) = \sqrt{k_0^2(\epsilon_r - 1) - k_z^2} \tag{19}$$

The resonant frequency ( $f_0$ ) can be calculated by resolving the equation for  $k_0$  in (1) The obtained normalized frequency will be:

$$F = \frac{2\pi a f_0 \sqrt{\epsilon_r}}{c} \tag{20}$$

#### 4. Results and Discussion

The resonant frequency is one of the significant parameter to decide the characteristics and performance of the antenna. Figure 2 plots the input characteristics of the antenna's S11 Vs frequency parameter. The return loss (RL) can be calculated:

$$RL = -10 \log_{10} |\rho|^2 = -20 \log_{10} |\rho| \text{ in dB} \tag{21}$$

where  $\rho$  is the return loss. The loss in the transmission line can be calculated by taking the difference between the excited power and the power delivered to the load.

$$P_{\text{loss}} = \frac{|V_0^+|^2}{2Z_0} (e^{2\omega l} - 1) + |\rho|^2 (1 - e^{-2\omega l}) \tag{22}$$

$(e^{2\omega l} - 1)$  is the loss of the incident wave and  $(1 - e^{-2\omega l})$  is the loss of the reflected wave. As shown the in the Figure 2, the impedance bandwidth of the DRA-I is found to be 12.43%, DRA-II has two bands. The impedance bandwidth of band-I and band-II are 4.81% and 5.87% respectively, DRA-III provides 10.8% impedance bandwidth. In this band VSWR is found to be less than 2.

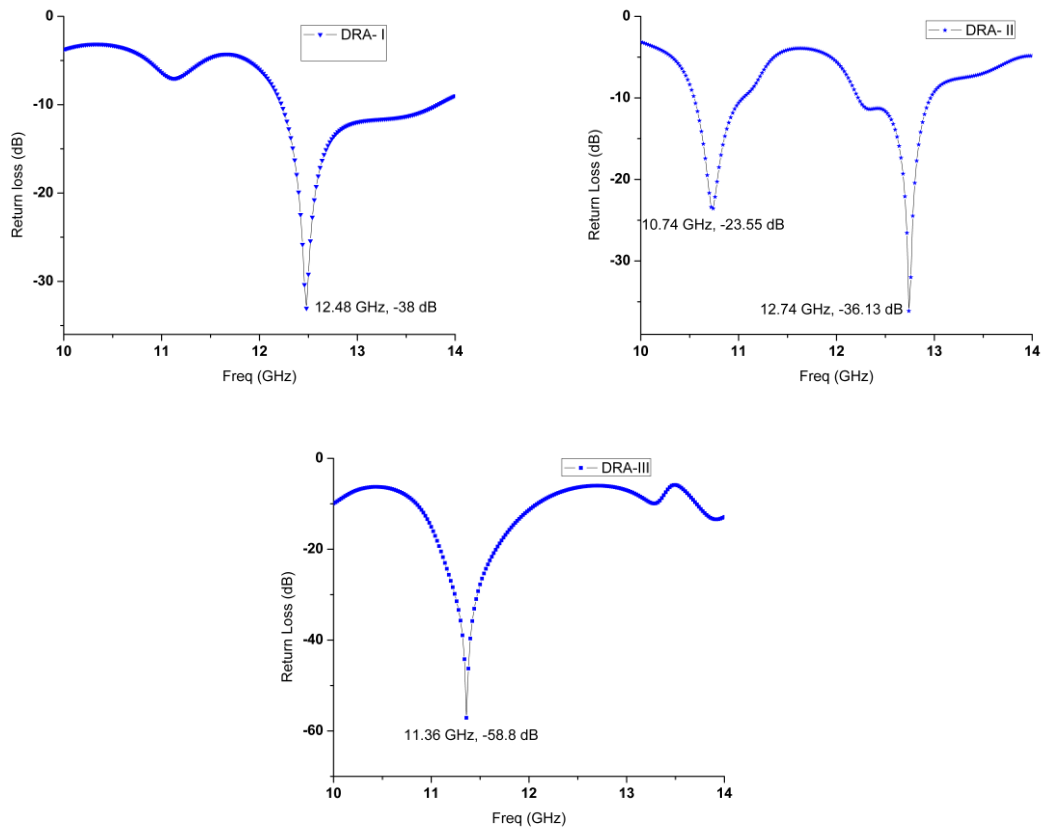


**Figure 2.** Plot of Return loss versus frequency in DRA-I, DRA-II and DRA-III

Figure 3 shows the resistive and reactive parts of the input impedance for all three designs. The changes along the microstrip line especially when it is within the aperture's initial or final edges. As shown in the figure resistive part of DRA-I increases initially from 10 GHz but after 10.5 GHz it settles down near to 50 Ohms. At near to 12 GHz, DRA-II shows peak input resistance but it also comes down with an increase in the frequency of operation. But DRA-III shows a smooth variation of the input resistance curve. The microstrip position can be used as fundamental parameters for matching and tuning the antenna. It is found that by appropriate matching the real impedance is around 50 ohm in the operating frequency band. Fig. 4 shows the output pattern in the E plane and H plane at the operating frequency of 12.4 GHz, 12.7 GHz, and 11.3 GHz by DRA-I, DRA-II, and DRA-III respectively.

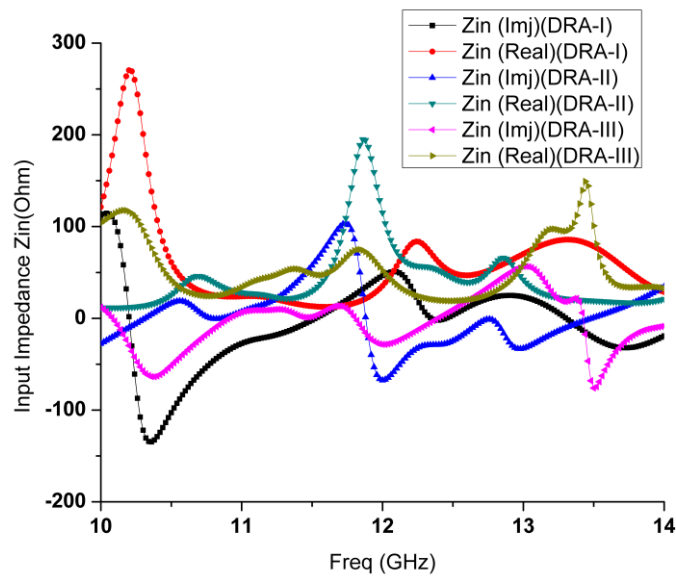


Figure 3. Plot of variation of the real and imj  $Z_{in}$ (Ohms) for DRA-I, DRA-II, and DRA-III with frequency.

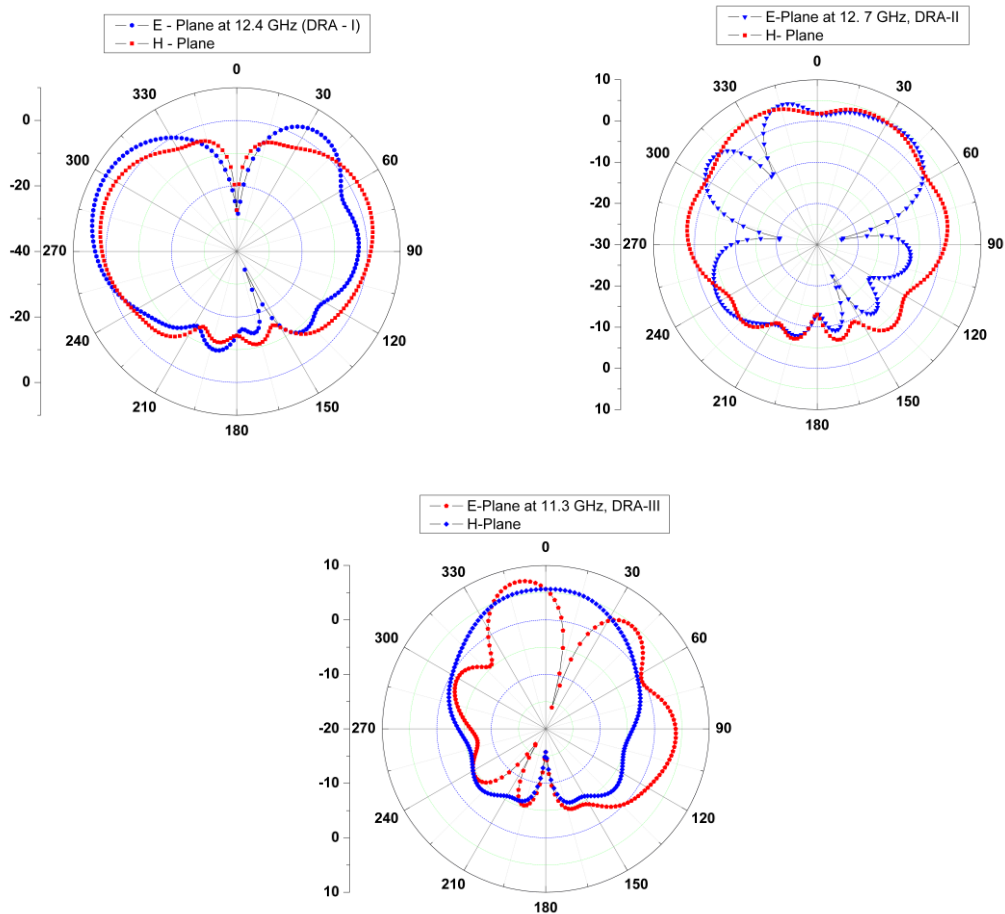
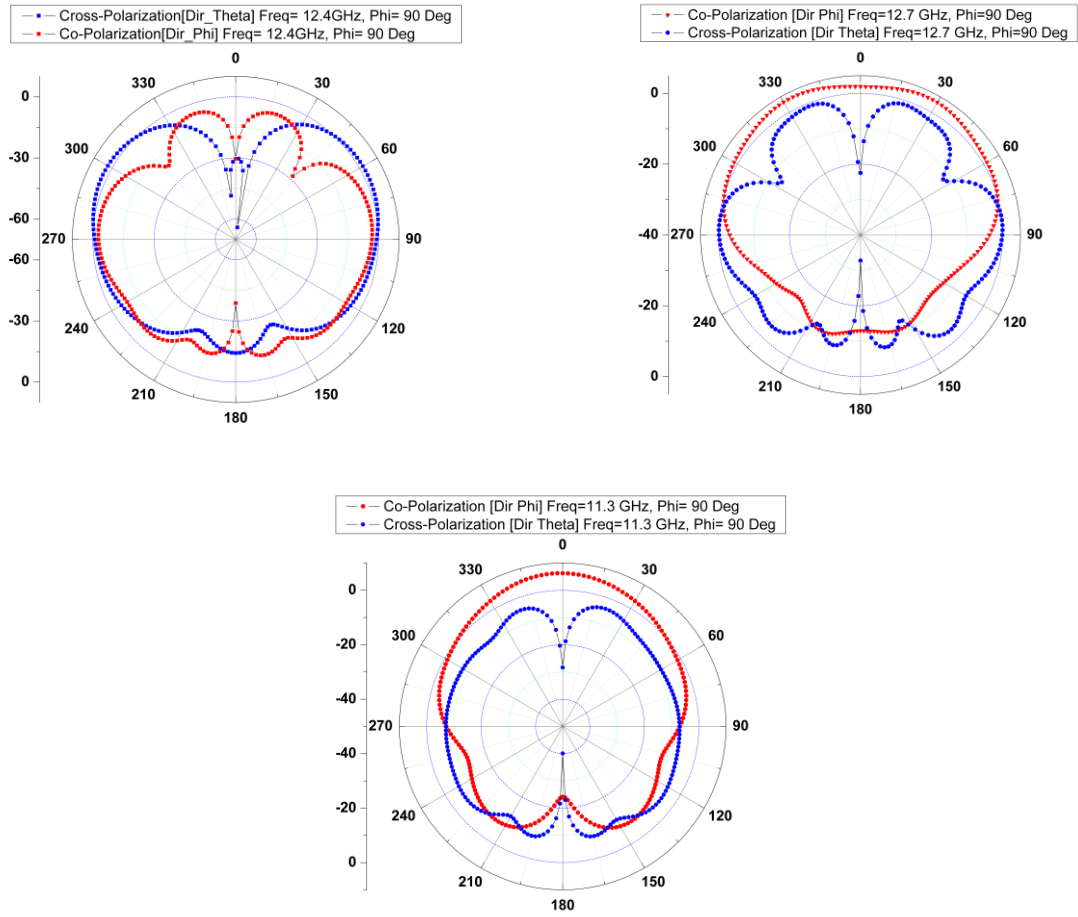
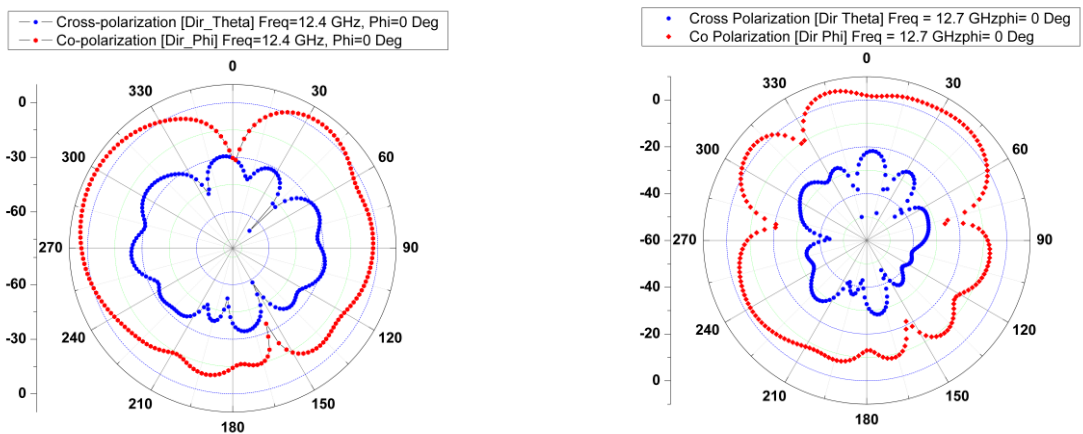


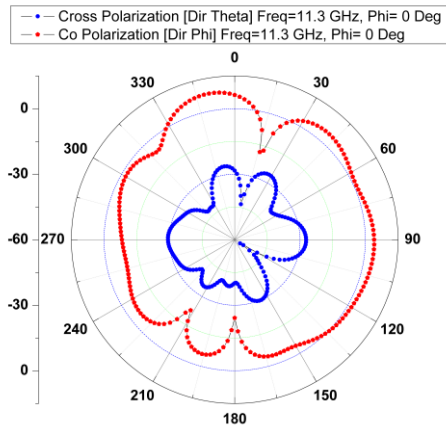
Figure4. Output pattern in E-plane and H-plane for DRA-I, DRA-II, and DRA-III



**Figure 5.** E-plane co and cross polarization of the DRA-I, DRA-II, and DRA-III.

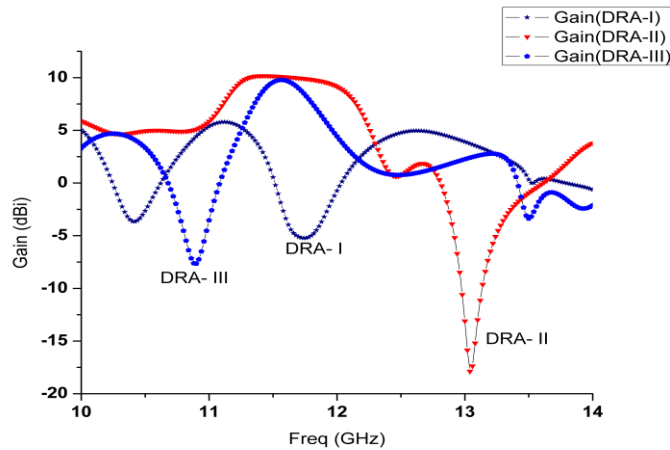
Fig. 5 shows the E-plane co and cross-polarization at 12.4 GHz, 12.7 GHz, and 11.3 GHz. The cross-polarization is unavoidable considering the practical aspect of the antenna. It has been observed that the difference between cross and co-polarization is more than 20 dB in the broadside direction for  $\theta = 0^\circ$  for DRA-II and III.





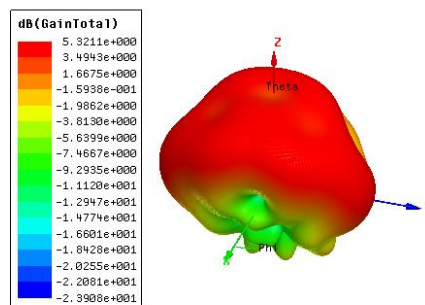
**Figure 6.** H-plane co and cross-polarization of the DRA-I, DRA-II, and DRA-III.

Fig. 6 shows the H-plane co and cross-polarization at 12.4 GHz, 12.7 GHz, and 11.3 GHz. The radiation pattern appears symmetric in H-plane. The difference between co and cross-polarization is seemed to be more than 30 dB.



**Figure 7.** Plot of gain versus frequency for DRA-I, DRA-II, and DRA-III.

Figure 7 indicates a comparative analysis of gain in dBi for all the three designs at their resonating frequency. DRA-II provides a peak gain of 9.8 dBi with maximum gain stability in its operating band. Figure 8 indicates the three-dimensional gain of DRA-II at 12.74 GHz. It is observed that in DRA-II a front-to-back ratio of 80.51 dB is obtained. Figure 9 shows the formation of surface current density (Amp/m<sup>2</sup>), electric field (Volt/m), and magnetic field (Amp/m) in DRA-II while operating at the resonant frequency.



**Figure 8.** 3-D Plot of gain in dB at 12.74 GHz of DRA-II

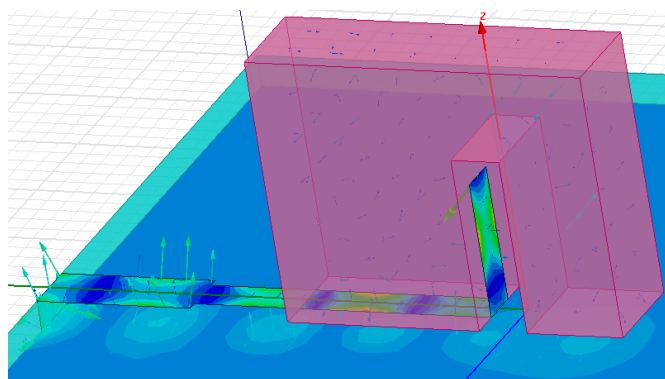


**Figure 9.** Formation of surface current density, E and H field on DRA-II at 12.74 GHz

**Table 2.** Performance analysis of DRA

	<b>DRA-I</b>	<b>DRA-II</b>	<b>DRA-III</b>
Maximum Resonating Frequency	12.48 GHz (-38 dB)	10.74 GHz (-23.55 dB) 12.74 GHz (-36.13 dB)	11.36 GHz(-58.8 dB)
Operating Band	12.22GHz to 13.84 GHz	Band-I: 10.54 to 11.06 GHz Band-II: 12.22 to 12.96 GHz	10.86 GHz to 12.1 GHz
Impedance Bandwidth (%)	12.43 %	Band-I: 4.81% Band-II: 5.87%	10.8%
Peak Directivity (dB)	7.25	7.28	7.25
Peak Gain (dBi)	7.24	7.32	7.24
Radiation Efficiency (%)	99.85%	100.52%	99.85%

## 5. Conclusion

Novel wideband, low-profile, high gain RDRA is proposed. The various microstrip inset feeding configuration shows that proposed antennas provide good impedance matching and stable radiation pattern in the entire frequency of operation. After comparing various parameters it is observed that DRA-II provides excellent input and output characteristics. This proposed antenna is a potentially suitable candidate for the vehicular radar system, imaging, near field communication system, etc.

## References

- [1]. Ramo, S., Whinnery, J. R., & Duzer, T. V. (1993). *Field and wave in communication electronics system*, Singapore: John Wiley & Sons.
- [2]. Harrington, R. F. (2001). *Time harmonic electromagnetic fields*, 445 Hoes Lane, Piscataway, NJ: IEEE Press.
- [3]. Waterhouse, R. B. (2003). *Microstrip Patch Antennas: A Designer's Guide*, Kluwer Academic Publishers, Massachusetts, USA.
- [4]. Pozar, D. M., & Schaubert, D. H. (1995). *Microstrip patch antennas: the analysis and design of microstrip antennas and arrays*, Wiley-IEEE Press.
- [5]. Luk, K. M., & Leung, K. W. (2003). *Dielectric resonator antennas*, Research Studies Press, Baldock, Hertfordshire, U.K.
- [6]. Mongia, R. K., & Ittipiboon, A. (1997). Theoretical and experimental investigations on rectangular dielectric resonator antennas, *IEEE transaction on antennas and propagation*, 45(9).
- [7]. Coulibaly, Y., & Denidni, T. A. (2008). Broadband micro-strip fed dielectric resonator antenna for X-band applications, *IEEE antenna and wireless propagation letters*, 7.
- [8]. Petosa, A. (2007). *Dielectric Resonator Antenna Handbook*, Norwood: Artech House.
- [9]. Garg, R. (2008). *Analytical and Computational Methods in Electromagnetics*, Norwood: Artech House.
- [10]. Yaduvanshi, R. S, Parthasarathy, H. (2016). *Rectangular Dielectric Resonator Antennas, Theory and Design*, New Delhi: Springer India.
- [11]. Mohanty, S., & Mohapatra, B. (2020). Leaky Wave-Guide Based Dielectric Resonator Antenna for Millimeter-Wave Applications, *Trans. Electr. Electron. Mater.*, <https://doi.org/10.1007/s42341-020-00240-w>.
- [12]. Mongia, R. K., & Ittipiboon, A. (1997). Theoretical and experimental investigations on rectangular dielectric resonator antennas, *IEEE transaction on antennas and propagation*, 45 (9).